JACS JOURNAL OF THE AMERICAN CHEMICAL SOCIETY

Communication

Cite This: J. Am. Chem. Soc. 2018, 140, 9797−9800

pubs.acs.org/JACS

Direct Synthesis of Colorful Single-Walled Carbon Nanotube Thin Films

Yongping Liao, Hua Jiang,* Nan Wei, Patrik Laiho, Qiang Zhang, Sabbir A. Khan, and Esko I. Kauppinen*

Department of Applied Physics, Aalto University School of Science, P.O. Box 15100, FI-00076 Aalto, Finland

Supporting Information

ABSTRACT: In floating catalyst chemical vapor deposition (FC-CVD), tuning chirality distribution and obtaining narrow chirality distribution of single-walled carbon nanotubes (SWCNTs) is challenging. Herein, by introducing various amount of CO_2 in FC-CVD using CO as a carbon source, we have succeeded in directly synthesizing SWCNT films with tunable chirality distribution as well as tunable colors. In particular, with 0.25 and 0.37 volume percent of CO_2, the SWCNT films display green and brown colors, respectively. We ascribed various colors to suitable diameter and narrow chirality distribution of SWCNTs. Additionally, by optimizing reactor temperature, we achieved much narrower (n,m) distribution clustered around (11,9) with extremely narrow diameter range (>98% between 1.2 and 1.5 nm). We propose that CO_2 may affect CO disproportionation and nucleation modes of SWCNTs, resulting in SWCNTs' various diameter ranges. Our work could provide a new route for high-yield and direct synthesis of SWCNTs with narrow chirality distribution and offer potential applications in electronics, such as touch sensors or transistors.

Single-walled carbon nanotubes (SWCNTs) have attracted massive attention owing to their exceptional structural and electronic properties.[1−4] Because the electronic and optical properties of SWCNTs critically depend on their chirality, it is important to achieve SWCNTs with narrow chirality distributions. Typically, there are two main approaches to obtain SWCNTs with narrow chirality distribution: direct growth and postsynthesis purification. The postsynthesis purification method is primarily based on a solution process, such as ion-exchange chromatography separation (IEX) of DNA-wrapped SWCNTs,[5] density gradient ultracentrifugation (DGU),[6] gel chromatography[7] and aqueous two-phase separation techniques.[8] However, the chemicals and sonication process in solution may result in contamination and might damage the nanotubes. On the other hand, direct growth of SWCNTs with narrow chirality distribution can retain their intrinsic properties. Such methods include the use of CNT segments as seeds,[9] the growth initiated from carbonaceous molecular seeds[10] and the use of well-designed catalysts for (n,m)-selective growth.[11−15] However, these approaches are limited by the low yield and difficulties of preparing CNT segments or catalysts.

Floating catalyst chemical vapor deposition (FC-CVD),[16,17] nevertheless, as a continuous process, allows a high-yield production of SWCNTs with high quality. In addition, SWNCTs can be directly collected onto a membrane filter to form a thin film for further applications with no need of pretreatment. However, because catalyst nanoparticles are without support in aerosol environment,[18] a more complex evolution of catalysts may bring up a big challenge to selectively grow SWCNTs with narrow chirality distribution in FC-CVD. Zhu et al. reported that an appropriate amount of NH_3 can narrow the chirality distribution in a FC-CVD produced SWCNTs.[19] However, SWCNTs could be doped by N due to the existence of NH_3 at high temperature. The alien atom like nitrogen may alter the electrical properties of SWCNTs.

Here, we report a novel method for the direct growth of SWCNTs with tunable colors and narrow-chirality distribution by introducing a certain amount of CO_2 in the FC-CVD process. Further, we demonstrated that the colors correlate strongly to both the diameter and the chirality distribution of the SWCNTs.

SWCNTs were synthesized using CO as carbon source with a flow rate of 350 ccm, and ferrocene as catalyst precursor carried by 50 ccm CO flow. To tune the growth of SWCNTs, various amount of CO_2 with flow rates of 0, 1, 1.5, and 2.0 ccm, corresponding volumetric fractions of 0, 0.25, 0.37, and 0.50 vol %, respectively, were introduced into the reactor at 850 or 880 °C. The experimental details and schematic of the FC-CVD reactor were illustrated in Supporting Information (Figure S1).

Obviously, the SWCNT thin films produced with various CO_2 concentrations display different colors (Figure 1a, the camera setting is shown in Supporting Information). Particularly, the thin films with CO_2 concentration of 0.25 and 0.37 vol % display green and brown color, respectively. The (scanning) transmission electron microscopy ((S)TEM) and energy dispersive spectroscopy show that our thin films possess high purity and these samples have similar nanoparticle contents and size distributions (Figure S2 and S13), implying that the nanoparticle contents do not account for the color variations in our SWCNT thin films. With an increase of CO_2 concentration, the transition peaks S11 and S22 from semiconducting tubes have an obvious redshift (Figure 1b). From Kataura plot, we calculated the mean diameter of

Received: May 16, 2018
Published: July 26, 2018

DOI: 10.1021/jacs.8b05151
J. Am. Chem. Soc. 2018, 140, 9797−9800

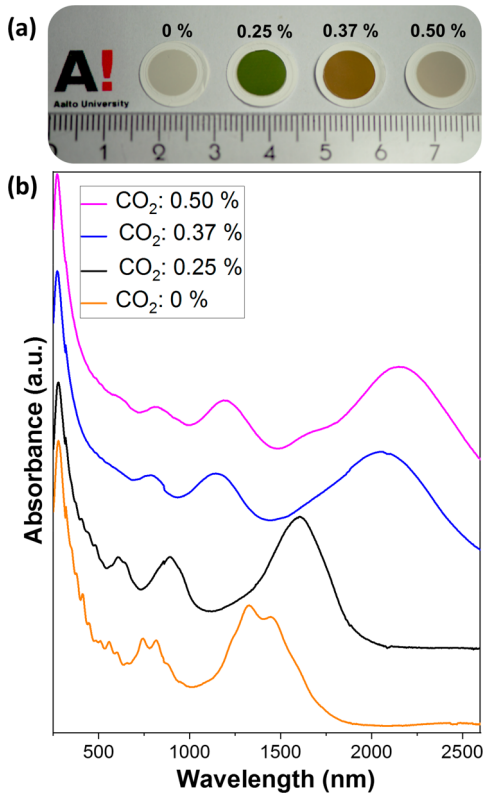

Figure 1. (a) Optical image of SWCNT thin films on filters obtained from different CO_2 concentration at 850 °C and (b) corresponding absorption spectra.

SWCNTs. For CO_2 concentration of 0, 0.25, 0.37, and 0.50 vol %, the corresponding mean diameters of SWCNTs are about 1.1, 1.3, 1.8, and 1.9 nm, respectively. The radial breathing modes of Raman spectra also identify the increment of SWCNT diameter (Figure S3).

It is reasonable to correlate the colors of the SWCNT films to their structural properties and absorption features. Because of the various diameter distribution of SWCNTs, the transition peaks M11 from metallic tubes may also shift. The color of the film is mainly attributed to the sharp absorption peaks in the visible region, for instance, the green film (0.25 vol % CO_2) displays a distinct and sharp absorption peak (M11) at a wavelength of approximately 610 nm (Figure 1b and Figure S4). The brown film (0.37 vol % CO_2) mainly results from the relatively flatter M11 peak at about 760 nm. Other samples with no obvious absorption peaks (0.50 vol % CO_2) or very weak peaks (0 vol % CO_2) in the visible region display a normal gray color. Similar phenomena were found by Hersam et al. using the DGU method.[20] To the best of our knowledge, this is the first time direct synthesis of SWCNT films with specific colors has been reported.

To further understand the chiral structure distributions of SWCNTs in the produced samples, electron diffraction analysis of both the individual and bundled nanotubes was carried out using a TEM. Figure 2 shows a high-resolution TEM image of an individual SWCNT (a) and its corresponding electron diffraction patterns (EDP) (b). Based on an intrinsic layerline spacing analysis method[21] from the EDP in Figure 2b, the (n,m) of this individual nanotube has been indexed as (16,13). More EDPs of individual SWCNT with 0.25 vol % CO_2 can be found in Figure S5, the typical

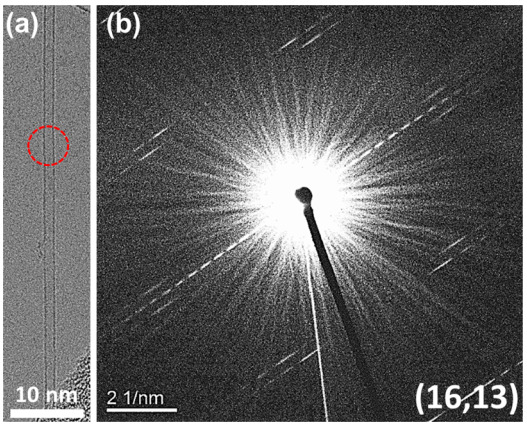

Figure 2. (a) Typical TEM image of an individual SWCNT and (b) its corresponding electron diffraction pattern with CO_2 concentration of 0.50 vol % at 850 °C.

TEM images and EDPs of SWCNTs with 0 vol % and 0.25 vol % are shown in Figure S6. Statistically, the (n,m) maps based on electron diffraction analysis from around 120 individual tubes for all investigated samples are shown in Figure 3a–c. The exact number of each (n,m) is available in Figure S7.

Obviously, the mean diameter of nanotubes increases with the CO_2 concentration (Figure 3a–d), which is consistent with the absorption results. Notably, the SWCNTs with 0.25 vol % CO_2 possess much narrower diameter (1.0–1.5 nm) and chirality distribution compared to those with 0 vol % and 0.50 vol %. Because of the proper diameter and narrow chirality

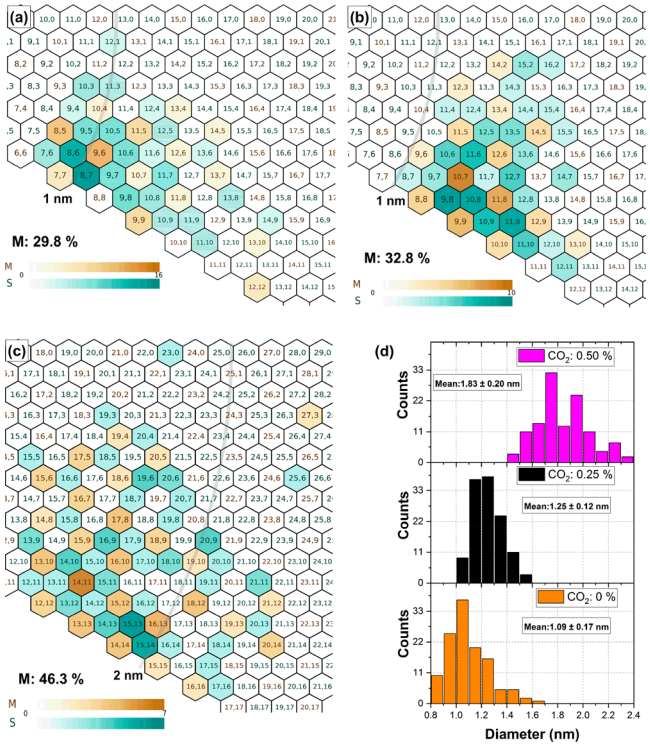

Figure 3. Chirality distribution of individual SWCNTs with CO_2 concentration of (a) 0 vol %, (b) 0.25 vol %, and (c) 0.50 vol % at 850 °C. The insets represent the number of metallic and semiconducting tubes. (d) Diameter distribution of individual SWCNTs summarized from (n,m) maps with different CO_2 concentration.

DOI: 10.1021/jacs.8b05151
J. Am. Chem. Soc. 2018, 140, 9797–9800

distribution for SWCNTs with 0.25 vol % CO_2, a dominant and sharp absorption peak is observed in the visible region (~610 nm), leading to the green color (Figure 1). On the other hand, with a broader chirality distribution in SWCNTs with 0 or 0.50 vol % CO_2, only weak peaks are observed in the visible region, resulting in the normal gray color. In addition, the chiral angle distributions of individual nanotubes are displayed in Figure S9a−c. All three samples display a preferable chiral angle between 20° and 30° (~80%), which may result from the thermodynamic stability of near armchair tubes, as well as the promoted growth kinetics aided by the kinks at tube edges for the chiral tubes.[22]

To investigate the electronic structure of SWCNT bundles, we also performed the EDPs of SWCNT bundles. By analyzing the relationship of diffraction layerlines from all individual SWCNTs in a bundle,[23] it was uncovered that the bundle is composed of nanotubes with three different chiral angles of 3.1°, 18.9°, 26.1° (Figure S8a,b). It turns out that the chiral angle distribution of the bundles exhibits a similar trend to individual tubes (Figure S9a−f), implying the identical global chiral angle distributions over the SWCNTs.

In addition, the metallic tube ratio increases from 29.8 to 46.3% when increasing CO_2 concentration from 0 to 0.50 vol % (Figure 3a−c). Further increasing CO_2 concentration to 1.23 vol %, however, degrades the quality of SWCNTs (Figure S10).

Temperature also plays an important role in selective growth of SWCNTs with narrow chirality distribution.[24] Higher temperature can reduce decomposition of CO, leading to a more controllable synthesis toward narrow chirality distribution. Figure 4 shows the (n,m) distribution and diameter

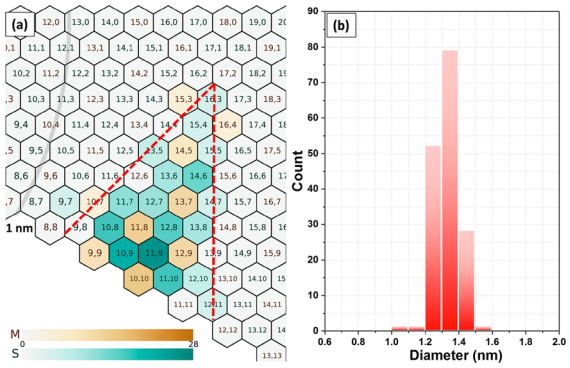

Figure 4. (a) Chirality and (b) diameter distribution of SWCNTs with 0.25 vol % CO_2 at 880 °C.

histogram of SWCNTs synthesized with 0.25 vol % CO_2 at 880 °C. Apparently, compared with SWCNTs produced at 850 °C, much narrower chirality distribution clustered around (11,9) (~17%) was obtained (total 162 tubes). The number of each chirality can be found in Figure S11. In particular, the SWCNTs present a very narrow diameter distribution with the majority (>98%) in the range of 1.2−1.5 nm (Figure 4b). Remarkably, our tubes have a mean diameter of 1.35 nm, which is larger than those of HiPco[25] or CoMoCAT[15] (~0.8 nm). Furthermore, SWCNTs with various diameter can satisfy different applications, for example as a laser absorber,[26] and these colorful SWCNT films show high conductivity (Figure S12), which may have great potential applications in touchscreens.

The role of CO_2 is yet unclear. It has been reported that CO_2 may etch the small-diameter SWCNTs, which are more active than the large-diameter ones.[26] However, on the basis of our chirality analysis, it is hard to conclude that CO_2 may etch SWCNTs. For instance, in the sample without CO_2, the SWCNTs distribute in the small diameter range from 0.9 to 1.5 nm, but when we introduced 0.50 vol % CO_2, the chirality distribution became broader, spanning 1.5−2.3 nm (Figure 3a,c). Furthermore, it has also been considered that metallic tubes are more active than semiconducting tubes, implying that the metallic tubes could be etched away more easily by an etchant.

Though our results are contradictory, they show that the metallic ratio actually increases with the assistance of CO_2. Therefore, our results suggested that the role of CO_2 in FC-CVD production of SWCNTs remains veiled and requires further investigation. We prefer to postulate that a certain amount of CO_2 can affect CO disproportionation, as well as carbon dissolution and diffusion on a catalyst due to the removal of amorphous carbon from the catalyst by CO_2. Hence, the nucleation modes of SWCNTs could also be affected, the tangential or perpendicular modes may exist consequently, resulting in different SWCNT diameters.[27] By measuring the size of catalysts with TEM (Figure S13), we found that the catalyst size distribution with 0 vol % CO_2 is similar to that with 0.50 vol % (~2.7 nm), whereas the diameter of an as-grown SWCNT on a catalyst differs from each other according to results in Figure 3. This indicates that without adding CO_2, SWCNTs may prefer to grow in a perpendicular mode, leading to small diameter tubes. With the proper amount of CO_2, SWCNTs may grow in a tangential or near-tangential mode, which results in larger diameter tubes.

In summary, we have succeeded in the direct synthesis of colorful SWCNT thin films using a conventional FC-CVD process by introducing a certain amount of CO_2. By controlling the flow rate of CO_2 and optimizing the reaction conditions, the color of the SWCNT thin films can be tuned from gray, green, brown to gray. The colors of the SWCNT thin films are attributed to nanotube diameter distributions in particular ranges that give rise to absorption peaks in the visible region. The narrow (n,m) chirality distribution also accounts for the display of a certain color of a SWCNT thin film. We also found that the ratio of metallic tubes increases with the CO_2 concentration. The color-tunable SWCNT films promise such potential applications as building blocks in touch sensors with a friendly human−machine interface and in high-performance transistors.

■ ASSOCIATED CONTENT

Supporting Information

The Supporting Information is available free of charge on the ACS Publications website at DOI: 10.1021/jacs.8b05151.

Experimental details, schematic of reactor, more TEM and EDPs, statistics of chirality, chiral angle distribution, Raman spectra, sheet resistance, catalyst size distribution (PDF)

■ AUTHOR INFORMATION

Corresponding Authors

*esko.kauppinen@aalto.fi
*hua.jiang@aalto.fi

DOI: 10.1021/jacs.8b05151
J. Am. Chem. Soc. 2018, 140, 9797−9800

ORCID

Yongping Liao: 0000-0002-6146-9481
Patrik Laiho: 0000-0001-8234-1607
Sabbir A. Khan: 0000-0003-1279-7638

Notes

The authors declare no competing financial interest.

■ ACKNOWLEDGMENTS

This work was funded by the 604472 (IRENA) and the AEF through the MOPPI project. The research has also been partially supported by the 286546 (DEMEC) and 292600 (SUPER) as well as 3303/31/2015 (CNT-PV) and 1882/31/2016 (FEDOC). This work made use of the Aalto-NMC premises.

■ REFERENCES

(1) Smalley, R. E. In *Carbon Nanotubes: Synthesis, Structure, Properties, and Applications*; Dresselhaus, M. S.; Dresselhaus, G.; Avouris, P., Eds.; Springer Science & Business Media, 2003; Vol. *80*.
(2) Jeon, I. I.; Cui, K.; Chiba, T.; Anisimov, A.; Nasibulin, A. G.; Kauppinen, E. I.; Maruyama, S.; Matsuo, Y. *J. Am. Chem. Soc.* **2015**, *137*, 7982.
(3) Jeon, I. I.; Chiba, T.; Delacou, C.; Guo, Y.; Kaskela, A.; Reynaud, O.; Kauppinen, E. I.; Maruyama, S.; Matsuo, Y. *Nano Lett.* **2015**, *15*, 6665.
(4) Jeon, I. I.; Seo, S.; Sato, Y.; Delacou, C.; Anisimov, A.; Suenaga, K.; Kauppinen, E. I.; Maruyama, S.; Matsuo, Y. *J. Phys. Chem. C* **2017**, *121*, 25743.
(5) Zheng, M.; Diner, B. A. *J. Am. Chem. Soc.* **2004**, *126*, 15490.
(6) Arnold, M. S.; Green, A. A.; Hulvat, J. F.; Stupp, S. I.; Hersam, M. C. *Nat. Nanotechnol.* **2006**, *1*, 60.
(7) Liu, H.; Nishide, D.; Tanaka, T.; Kataura, H. *Nat. Commun.* **2011**, *2*, 309.
(8) Khripin, C. Y.; Fagan, J. A.; Zheng, M. *J. Am. Chem. Soc.* **2013**, *135*, 6822.
(9) Liu, J.; Wang, C.; Tu, X.; Liu, B.; Chen, L.; Zheng, M.; Zhou, C. *Nat. Commun.* **2012**, *3*, 1199.
(10) Sanchez-Valencia, J. R.; Dienel, T.; Gröning, O.; Shorubalko, I.; Mueller, A.; Jansen, M.; Amsharov, K.; Ruffieux, P.; Fasel, R. *Nature* **2014**, *512*, 61.
(11) Yang, F.; Wang, X.; Zhang, D.; Yang, J.; Luo, D.; Xu, Z.; Wei, J.; Wang, J.-Q.; Xu, Z.; Peng, F.; Li, X.; Li, R.; Li, Y.; Li, M.; Bai, X.; Ding, F.; Li, Y. *Nature* **2014**, *510*, 522.
(12) Li, X.; Tu, X.; Zaric, S.; Welsher, K.; Seo, W. S.; Zhao, W.; Dai, H. *J. Am. Chem. Soc.* **2007**, *129*, 15770.
(13) Chiang, W.-H.; Sankaran, R. M. *Nat. Mater.* **2009**, *8*, 882.
(14) He, M.; Chernov, A. I.; Fedotov, P. V.; Obraztsova, E. D.; Sainio, J.; Rikkinen, E.; Jiang, H.; Zhu, Z.; Tian, Y.; Kauppinen, E. I.; et al. *J. Am. Chem. Soc.* **2010**, *132*, 13994.
(15) Bachilo, S. M.; Balzano, L.; Herrera, J. E.; Pompeo, F.; Resasco, D. E.; Weisman, R. B. *J. Am. Chem. Soc.* **2003**, *125*, 11186.
(16) Moisala, A.; Nasibulin, A. G.; Brown, D. P.; Jiang, H.; Khriachtchev, L.; Kauppinen, E. I. *Chem. Eng. Sci.* **2006**, *61*, 4393.
(17) Mustonen, K.; Laiho, P.; Kaskela, A.; Zhu, Z.; Reynaud, O.; Houbenov, N.; Tian, Y.; Susi, T.; Jiang, H.; Nasibulin, A. G.; et al. *Appl. Phys. Lett.* **2015**, *107*, 013106.
(18) Nikolaev, P.; Bronikowski, M. J.; Bradley, R. K.; Rohmund, F.; Colbert, D. T.; Smith, K.; Smalley, R. E. *Chem. Phys. Lett.* **1999**, *313*, 91.
(19) Zhu, Z.; Jiang, H.; Susi, T.; Nasibulin, A. G.; Kauppinen, E. I. *J. Am. Chem. Soc.* **2011**, *133*, 1224.
(20) Green, A. A.; Hersam, M. C. *Nano Lett.* **2008**, *8*, 1417.
(21) Jiang, H.; Nasibulin, A. G.; Brown, D. P.; Kauppinen, E. I. *Carbon* **2007**, *45*, 662.
(22) Artyukhov, V. I.; Penev, E. S.; Yakobson, B. I. *Nat. Commun.* **2014**, *5*, 4892.
(23) Jiang, H.; Brown, D.; Nikolaev, P.; Nasibulin, A. G.; Kauppinen, E. I. *Appl. Phys. Lett.* **2008**, *93*, 141903.
(24) Li, P.; Zhang, X.; Liu, J. *Chem. Mater.* **2016**, *28*, 870.
(25) Bachilo, S. M.; Strano, M. S.; Kittrell, C.; Hauge, R. H.; Smalley, R. E.; Weisman, R. B. *Science* **2002**, *298*, 2361.
(26) Tian, Y.; Timmermans, M. Y.; Kivistö, S.; Nasibulin, A. G.; Zhu, Z.; Jiang, H.; Okhotnikov, O. G.; Kauppinen, E. I. *Nano Res.* **2011**, *4*, 807.
(27) Fiawoo, M.-F.; Bonnot, A.-M.; Amara, H.; Bichara, C.; Thibault-Pénisson, J.; Loiseau, A. *Phys. Rev. Lett.* **2012**, *108*, 195503.

DOI: 10.1021/jacs.8b05151
J. Am. Chem. Soc. 2018, 140, 9797−9800